LAWRENCE
LIVERMORE
NATIONAL
LABORATORY

LLNL-JRNL-468333

LR: Compact connectivity representation for triangle meshes

T. Gurung, M. Luffel, P. Lindstrom, J. Rossignac

January 31, 2011

ACM Transactions on Graphics

Disclaimer

LR: Compact Connectivity Representation for Triangle Meshes

Topraj Gurung*
Georgia Institute of Technology

Mark Luffel†
Georgia Institute of Technology

Peter Lindstrom‡
Lawrence Livermore National Laboratory

Jarek Rossignac§
Georgia Institute of Technology

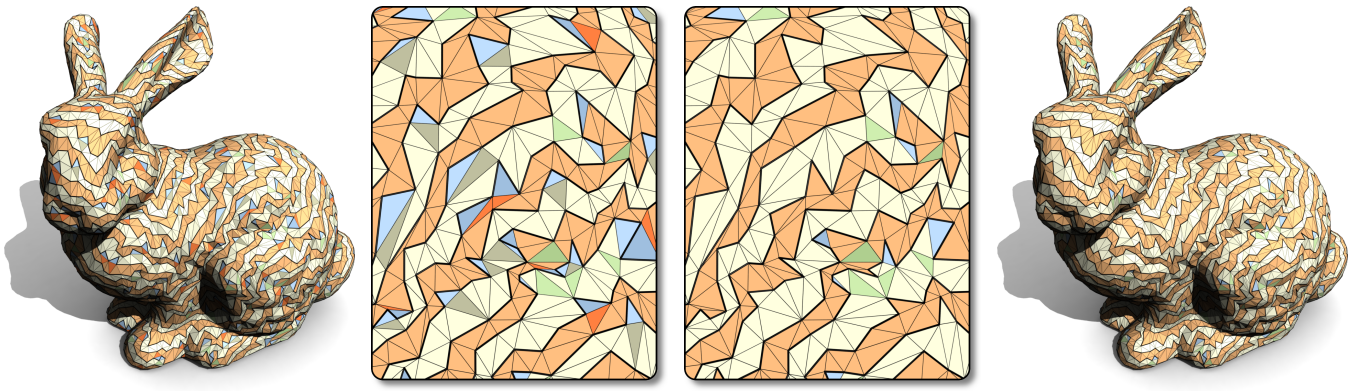

Figure 1: *The ring (black loop) delineates two corridors of triangles. Normal T_1 triangles (cream/orange) have one ring edge, dead-end T_2 triangles (blue) have two ring edges, and T_0 triangles (green) comprising bifurcations have no ring edges. Adjacent T_0 (gray/red) and T_2 triangles (left) are represented internally as inexpensive T_1 triangles (right), thereby significantly reducing storage. Our LR representation supports random access to connectivity, storing on average only 1.08 references or 26.2 bits per triangle.*

Abstract

We propose LR (*Laced Ring*)—a simple data structure for representing the connectivity of manifold triangle meshes. LR provides the option to store on average either 1.08 references per triangle or 26.2 bits per triangle. Its construction, from an input mesh that supports constant-time adjacency queries, has linear space and time complexity, and involves ordering most vertices along a nearly-Hamiltonian cycle. LR is best suited for applications that process meshes with fixed connectivity, as any changes to the connectivity require the data structure to be rebuilt. We provide an implementation of the set of standard random-access, constant-time operators for traversing a mesh, and show that LR often saves both space and traversal time over competing representations.

CR Categories: I.3.5 [Computer Graphics]: Computational Geometry and Object Modeling—Boundary representations

Keywords: triangle meshes, mesh connectivity, Hamiltonian cycle

Links: DL PDF

*e-mail: topraj@cc.gatech.edu
†e-mail: mluffel@cc.gatech.edu
‡e-mail: pl@llnl.gov
§e-mail: jarek@cc.gatech.edu
Prepared by LLNL under Contract DE-AC52-07NA27344.

1 Introduction

Compact triangle mesh representations that support random access are of increasing importance, given the rising complexity of meshes handled by applications and the proliferation of mobile and multi-core architectures. Compact representations help to reduce 1) the frequency of page faults, 2) the cost of swapping mesh portions between processors, and 3) the amount of memory required for storing a complete scene on a GPU or game console.

Our contributions are best explained as a storage-saving modification of the Corner Table (CT) [Rossignac 2001], which for each triangle stores 3 integer references to its vertices in the V table and 3 references to opposite corners in adjacent triangles in the O table. In contrast, the LR (*Laced Ring*) representation proposed here for manifold triangle meshes with fixed connectivity can be used to reduce storage for the connectivity information to either about 1.08 rpt (references per triangle) or to only about 26.2 bpt (bits per triangle), based on averaging the storage costs for our benchmark models. In a CT representation with 32-bit references and 16-bit vertex coordinates, the connectivity accounts for 90% of the total storage cost. LR does not require any particular compression of the vertex geometry, but we assume that memory-constrained applications will favor 16-bit coordinates. Under these conditions, using LR instead of CT results in a 75% reduction in total storage.

In spite of its compactness, LR supports the full set of standard random-access operators, including all those supported by CT, plus the vertex-to-incident-triangle (star) reference. These operators provide random access from an element (vertex, edge, or triangle) to adjacent elements, and permit visiting the vertices of a triangle and the triangles or edges incident upon a vertex in the cyclic order defined by the orientation of the mesh. We provide the details of a practical and efficient implementation of these operators, which each have constant-time complexity.

This significant progress over prior art builds on the following novel contributions.

Ring-based ordering: We build a nearly-Hamiltonian cycle of primal mesh edges that we call the **ring**. It divides the mesh in two parts (Fig. 1) that form triangle strip corridors with bifurcations. To reduce storage, we classify triangles by the number of edges they have on the ring (**bifurcation** T_0, **normal** T_1, **dead-end** T_2). We store the ring vertices and the T_1 and T_2 triangles in the order in which they are visited by the ring. The isolated vertices not part of the ring are stored last. The T_0 triangles are stored using the standard CT data structure.

Omitted V entries for T_1 and T_2 triangles: Most triangles are of type T_1 or T_2. Two of their vertex references (V entries of the CT) are defined implicitly and need not be stored. Thus, we store two references, $L[v]$ and $R[v]$, per ring vertex and assume that triangle $2v$ has vertices $(v, L[v], v.n)$ and triangle $2v+1$ has vertices $(v.n, R[v], v)$, where $v.n = (v+1) \bmod m_r$ is the next vertex after v on the ring, and where m_r denotes the number of ring vertices. Although this data structure has two entries for each T_2 triangle, the cost of this redundancy is amortized, because typically there are far fewer T_2 than T_1 triangles.

Omitted O entries for cheap T_1 and T_2 triangles: We do not store O table entries for the "cheap" T_1 and T_2 triangles that are not adjacent to a T_0, because we can access the opposite corners directly from neighboring ring vertices in constant time.

RING-EXPANDER construction of the ring: We propose a simple (linear time and space) greedy approach for computing a ring that, in all tested cases, either produces a Hamiltonian cycle or leaves a small proportion of isolated vertices. Our RING-EXPANDER algorithm tends to minimize the number of T_0 and T_2 triangles.

Wart skipping: To further reduce storage, we conceptually modify the ring to exclude **warts**—T_2 triangles adjacent to T_0 triangles—which allows the expensive T_0 triangles adjacent to warts to be represented as cheap T_1 triangles (Fig. 1).

Short offsets: When differences $|L[v] - v|$ and $|R[v] - v|$ are sufficiently small, we choose to store $L[v]$ and $R[v]$ as short 2-byte relative **offsets**. We provide a compact data structure for accommodating exceptions, when the offset is too large.

HYBRID-RING-EXPANDER for increased locality: For large meshes, LR provides the option of either minimizing the number of references or the number of bits stored. For the latter option, we provide a modified RING-EXPANDER that attempts to reduce the average magnitude of offsets.

2 Terminology and Notation

We assume a mesh with m vertices and n triangles. The vertices, which are numbered between 0 and $m-1$, are stored in a **geometry** table (array of points). The **connectivity** captures: (1) triangle/vertex **incidence**, (2) its reverse (**star**), (3) triangle/triangle and vertex/vertex **adjacency** (access to neighbors), and (4) **ordering** of vertices around triangles and of triangles around vertices.

Numerous data structures have been proposed for connectivity so as to support constant-time operators for traversing the mesh from one element (triangle or vertex) to adjacent ones in an orderly manner [Guibas and Stolfi 1985; Brisson 1989; Rossignac 1994].

When conventional data structures are used, the storage cost of the connectivity exceeds the storage cost of the geometry. Indeed, the triangle/vertex incidence alone amounts to 3 rpt and thus requires twice the storage of geometry, because in a manifold mesh with relatively low genus the number of triangles is roughly $2m$. Popular data structures use several additional references per triangle to encode adjacency, order, and other connectivity relationships.

$c.v$	vertex of corner c
$c.t$	triangle of corner c
$c.n$	next corner around $c.t$
$c.p$	previous corner around $c.t$
$c.s$	next corner around $c.v$
$c.o$	corner opposite of c
$c.l$	left neighbor $c.n.o$ of c
$c.r$	right neighbor $c.p.o$ of c
$v.c$	a corner of vertex v
$t.c$	a corner of triangle t

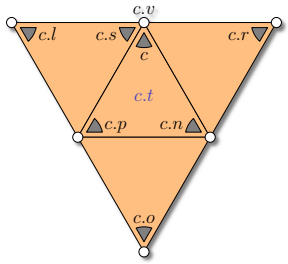

Figure 2: *Standard set of corner operators.*

2.1 Corner Table

We present our work in terms of **corners** [Rossignac 2001], which each associate a triangle with a bounding vertex. To facilitate comparison with prior art that manipulates **half-edges** (also called edge-uses or directed-edges) [Mantyla 1988; Campagna et al. 1998], we observe that each half-edge h corresponds to a unique **facing** corner c and that the next and opposite half-edge operators, $h.n$ and $h.o$, map to equivalent corner operators $c.n$ and $c.o$.

Fig. 2 shows the **standard corner operators**. Although corner and vertex references are stored in the LR data structure as integers, we use an object-oriented notation that interprets the operator based on the type of the operand. For example, if c is a corner, $c.n.v.n.c$ means: start with c, go to the next corner $c.n$ around the triangle $c.t$, obtain the reference $c.n.v$ to its vertex, go to the next vertex $c.n.v.n$ around the ring, and retrieve a corner $c.n.v.n.c$ of that vertex.

3 Prior Art

A customization of the popular **Winged-Edge** (**WE**) data structure [Baumgart 1972] to triangles stores connectivity using 3 references for each half-edge h: to its starting vertex $h.v$, to the opposite half-edge $h.o$, and to the next half-edge $h.n$ around the same triangle, resulting in a total of **9 rpt**.

As suggested by Campagna et al. [1998], the **Corner Table** (**CT**) data structure [Rossignac 2001] sorts the half-edge entries so that the three entries of a triangle are consecutive and listed in clockwise order (with respect to the outward pointing normal). This makes storing $c.n$ unnecessary, since it can be derived trivially using modular arithmetic. Hence, CT stores only two references per corner c: its **vertex** $c.v$ and its **opposite corner** $c.o$; see Fig. 2. CT uses two arrays V and O of integers so that $c.v = V[c]$ and $c.o = O[c]$.

WE and CT do not store any vertex-to-triangle references. One may add these by storing, for each vertex v, a reference $v.c = C[v]$ to one of its corners in the C table. Since there are three corners (and half-edges) per triangle and about twice as many triangles as vertices, with this addition, WE stores **9.5 rpt**, while CT stores **6.5 rpt**.

The mesh connectivity is completely captured in the V array of per-triangle vertex references and may be compressed to less than two bits per triangle [Rossignac 1999; Khodakovsky et al. 2002]. However, compressed formats produced through sequential encoding cannot be used for random access mesh traversal, and V alone does not provide constant-time access to neighboring elements. Some formats support local decompression [Yoon and Lindstrom 2007; Courbet and Hudelot 2009], but restrict the access pattern to a hierarchical or contiguous traversal and execute a complex decompression code each time a new portion of the mesh is accessed.

Castelli-Aleardi et al. [2006b] prove that a succinct representation of the connectivity of planar triangulations of n triangles can be

obtained by forming clusters of $O(\log n)$ triangles and by using the connectivity of a cluster to index a catalog of pre-computed look-up tables from which results of connectivity operators may be extracted in constant time. They form groups of $O(\log n)$ clusters to reduce the cost of storing inter-cluster connectivity information. Although this theoretical formulation has not been fully implemented, a less succinct version restricted to simple catalogs has been explored [Castelli Aleardi et al. 2006a; Mebarki 2008].

The **Star-Vertices** of Kallmann and Thalmann [2001] use **3.5 rpt** to store for each vertex v a circularly ordered list of references to adjacent vertices w, each augmented with an index i that identifies the position of the reference to v in the list of w. Hence they store one such (w, i) pair per half-edge. Because i typically fits in a few bits, w and i can be packed into a single reference. An additional per-vertex reference locates the beginning of each vertex's list.

Blandford et al. [2005] use a representation similar to the Star-Vertices, but reduce storage by ordering vertices according to a k-d tree, which allows them to take advantage of a variable-length encoding of relative vertex indices. They report storage costs of about 5 bytes per triangle. Their representation supports vertex adjacency efficiently, but does not allow linear indexing of triangles and corners (e.g. triangles exist only as vertex tuples), and hence does not support constant-time evaluation of the standard corner operators.

Snoeyink and Speckmann [1999] orient all edges and partition them into three disjoint vertex-spanning trees so that each vertex (except the vertices of a seed triangle) has exactly one outgoing edge in each tree. For each vertex v, they store six references to vertices w so that (v, w, u) is a triangle of the mesh and (v, u) an outgoing edge from v. Their **Tripod** data structure uses **3 rpt**.

Gurung et al. [2011] start with the Corner Table, but avoid storing the vertex-to-corner $v.c$ reference by matching each vertex with a corner of one or two incident triangles. They order the triangles so that the reference to the triangle or quad (triangle pair) matched with vertex v may be trivially recovered from the index of v. Furthermore, they eliminate the need to store the V table, and recover $c.v$ by walking around the unknown vertex using the $c.s$ swing operator until they reach the triangle or quad corner matched with $c.v$. Finally, they avoid storing pointers between corners within a quad. For efficiency, instead of storing the partial content of the O table, they store the equivalent swing references in an S table using 4 entries per matched quad or triangle. Their **SQuad** representation stores slightly more than **2 rpt**. In contrast to SQuad, LR stores vertex references from which swing corners are inferred.

4 The LR Representation

In this and the following section, we outline the LR (Laced Ring) approach, describe its representation, and discuss its construction and use. We focus here on a simple representation aimed at minimizing the number of references per triangle. A variation aimed at minimizing the number of bits per triangle is discussed in Section 6.

4.1 Topological Domain

We assume that the triangle mesh is a connected manifold without borders. Meshes with borders can be converted to closed manifolds by adding a dummy vertex v and a fan of dummy triangles around v that are joined with the border edges. We discuss the implementation of borders further in Section 4.6. Non-manifold meshes that represent the boundary of a solid may be converted to pseudo-manifolds while minimizing vertex replication [Rossignac and Cardoze 1999], and as such can be represented compactly using our LR data structure.

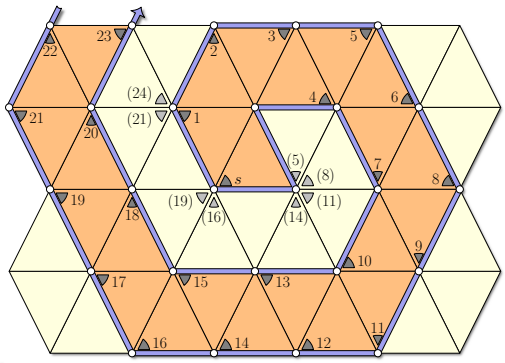

Figure 3: RING-EXPANDER *traversal. The corners are numbered in the order in which they are visited, starting with the seed* s.

4.2 The Ring

We first select and orient a manifold loop of mesh edges that visits most—and ideally all—vertices. We call it the **ring** and its edges the **ring edges**. The remaining edges are called **transversal**. Assume that the mesh has m vertices, out of which m_r vertices are on the ring. We want to minimize the number of **isolated vertices** $m_i = m - m_r$ that are not on the ring.

The perfect solution, i.e., a Hamiltonian cycle of edges, has been studied in graph theory. Unfortunately, previous studies of Hamiltonian cycles for triangle meshes are either focused on the dual graph, where the nodes represent triangles [Arkin et al. 1996; Gopi and Eppstein 2004], or are restricted to specific topologies and regular valence triangulations [Upadhyay 2010].

To construct the ring, we use the following greedy RING-EXPANDER algorithm. We begin by marking each triangle t and vertex v as unvisited by setting the flags $t.m$ and $v.m$ to false, respectively. We then pick a random **seed corner** s, from which we perform an invasion that visits most vertices and about half of the triangles. We ensure that the visited region is edge-connected, has no interior vertices (surrounded by all-visited triangles), and is bounded by a single manifold loop of edges (i.e., the ring). The RING-EXPANDER code, using corner operators, is simple:

```
c = s;                          // start at the seed corner s
c.n.v.m = c.p.v.m = true;   // mark vertices as visited
do {
    if (!c.v.m) c.v.m = c.t.m = true;     // invade c.t
    else if (!c.t.m) c = c.o;   // go back one triangle
    c = c.r;  // advance to next ring edge on the right
} while (c != s.o);       // until back at the beginning
```

RING-EXPANDER uses corner c to keep track of the current vertex $c.v$ and triangle $c.t$ being considered for invasion. The ring constructed so far separates the invaded triangles (orange) from the other ones (cream); see Fig. 3. If $c.v$ has not been visited, we invade triangle $c.t$, which has the effect of expanding the ring by replacing the ring edge facing c with the other two edges of the invaded triangle. Otherwise, if $c.v$ has been visited, we backtrack until we find a ring edge through which we may continue the invasion. This backtracking is accomplished without a stack or recursion by sliding along the ring ($c = c.o$) and by using the $t.m$ and $v.m$ flags as "breadcrumbs" to keep track of where we have been. These flags are stored efficiently in two bit vectors.

RING-EXPANDER's complexity is linear in space and time, since it visits each corner at most once. The construction is very fast, with a processing speed of around 30 million triangles per second.

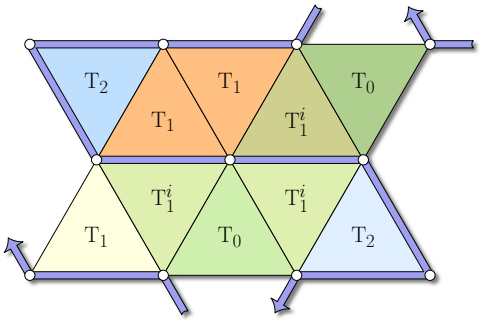

Figure 4: *Triangles are classified based on their number of ring edges and whether they are adjacent to a T_0 triangle.*

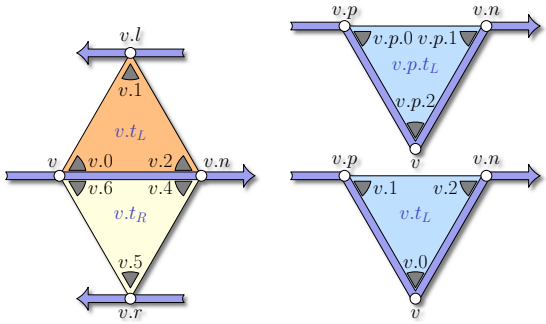

Figure 5: *Left: Left and right triangles $v.t_L$ and $v.t_R$ are defined for each ring edge $(v, v.n)$. Their corners are labeled $(v.0, v.1, v.2)$ and $(v.4, v.5, v.6)$. Right: Redundant (top) and canonical (bottom) representation of a T_2 triangle.*

In an attempt to minimize the number of isolated vertices m_i, we run RING-EXPANDER several times with random seed corners and retain the seed leading to the smallest m_i, which usually is negligible with respect to m and sometimes is zero. The first run yields a ratio m_i/m of 0.005% averaged over our test models. Additional runs often reduce this ratio.

4.3 Ring-based Classification of Triangles

To simplify exposition, we distinguish several kinds of triangles (see Fig. 4). T_0 triangles (bifurcations) have no ring edges; T_1 triangles (the most common kind) have exactly one ring edge each; T_2 triangles (dead-ends of the "corridors") have two edges on the ring. T_1^i and T_2^i are "expensive," **irregular** T_1 and T_2 triangles that share an edge with at least one T_0 triangle. Finally, we call a T_2 triangle that is adjacent to a T_0 triangle a **wart**. Such pairs of triangles are denoted T_0^w and T_2^w.

A triangle incident upon an isolated vertex must be T_0. Clearly a T_2 triangle cannot have an isolated vertex, since all of its three vertices are on the ring. Furthermore, a T_1 triangle has two consecutive ring vertices, v and $v.n$. If its third vertex w were isolated, then our construction algorithm would have included w in the ring between v and $v.n$, turning the triangle into a T_2.

4.4 Representing Incidence

We identify the ring vertices by integers between 0 and $m_r - 1$ assigned in order of appearance along the ring (starting from an arbitrary vertex). Hence, the references $v.p$ and $v.n$ to the vertices that respectively precede and follow v on the ring may be computed as $v.p = (v + m_r - 1) \bmod m_r$ and $v.n = (v + 1) \bmod m_r$. Vertices with indices between m_r and $m - 1$ are isolated vertices.

Each edge $e = (v, v.n)$ of the ring is associated with a starting vertex v and with two incident triangles: $v.t_L$ on the "left" and $v.t_R$ on the "right." We order the triangles so that $v.t_L = 2v$ and $v.t_R = 2v + 1$. Triangle $v.t_L$ has vertices $(v, v.l, v.n)$, where $v.l$ is stored in the L table as $L[v]$. Similarly, triangle $v.t_R$ has vertices $(v.n, v.r, v)$, where $v.r$ is stored in the R table as $R[v]$; see Fig. 5. T_0 triangles, which have no ring edges, are not stored in the LR table. Rather, they are represented in the regular Corner Table arrays V and O, and are assigned indices $2m_r$ and above.

We call the corners of the $v.t_L$ and $v.t_R$ triangles incident upon a ring edge the **ring corners**. We label them $v.0$, $v.1$, $v.2$, $v.4$, $v.5$, and $v.6$, as shown in Fig. 5, and assign to corner $v.i$ the integer index $8v + i$. Thus the **offset** i of a corner c is determined by the three least significant bits of c. By shifting the base of this scheme by eight rather than six for each vertex, we are not using corner IDs $8v + 3$ and $8v + 7$. This irregular assignment of indices speeds up some of the corner operators by allowing bit shifts and masks to be used in place of division and modulo. Although corners $8v + 3$ and $8v + 7$ do not exist, no storage is wasted on these unused indices, since we do not allocate space to each corner (except in the VO table; see below). Not using consecutive corner numbers limits the size of the mesh that can be stored, but using 32-bit references to opposite corners eliminates this concern for all practical purposes.

Note that there are two possible representations for the corners of a T_2 triangle: one for each of its two ring edges. For many traversal operations this is not a problem, but when unique corner references are desired, our convention is to associate the T_2 triangle with its second ring edge. We say that the other three corner references are **redundant**. We can easily detect that a reference is redundant and convert it to the corresponding canonical reference. For example, given a corner $c = v.p.2$ (see Fig. 5, top right), we detect that c is redundant because $v.p.l = v.n$, and compute the canonical corner reference as $v.0$. Mappings of other corners in this and in the symmetric configuration are handled similarly.

We can obtain a reference $v.c$ to a corner of a ring vertex v as $v.c = v.0 = 8v$ and visit the triangles incident on v using the $c.s$ operator. A reference to one corner of each isolated vertex is stored explicitly in an auxiliary array C.

If all the vertices were on the ring and if all the triangles were incident upon at least one edge of the ring, this representation would suffice to support all the standard corner operators, and would store only two references per vertex, or **1 rpt** (since there are roughly twice as many triangles as vertices).

4.5 Representing Adjacency

Triangle adjacency is provided by the opposite corner operator $c.o$. Within a **quad** formed by triangles $v.t_L$ and $v.t_R$, $v.1$ and $v.5$ are opposites. Hence $v.1.o$ and $v.5.o$ can be determined directly. In a T_2 triangle, $v.2.o$ and $v.4.o$ may be obtained by first remapping $v.2$ and $v.4$ to their redundant counterparts $v.p.1$ and $v.p.5$, and then computing their in-quad opposites (see Figs. 5 and 6).

Opposites that do not lie in a T_0 can be obtained for T_1 and T_2 corners $v.0$, $v.2$, $v.4$, and $v.6$ by visiting nearby vertices on the ring. That is, when crossing a transversal edge via $c.o$, one or both of the other edges in the adjacent T_1 or T_2 triangle must be ring edges. For instance, if $v.n.l = v.l$, then $v.0.o = v.n.2$. Otherwise, $v.l.p.l = v.n$ and $v.0.o = v.l.p.0$; see Fig. 6. When $c.o$ lies in a T_2 triangle, we must also remap the corner in case it is redundant.

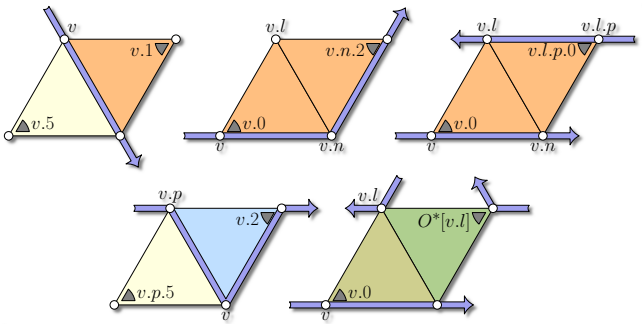

Figure 6: *Different cases for computing c.o.*

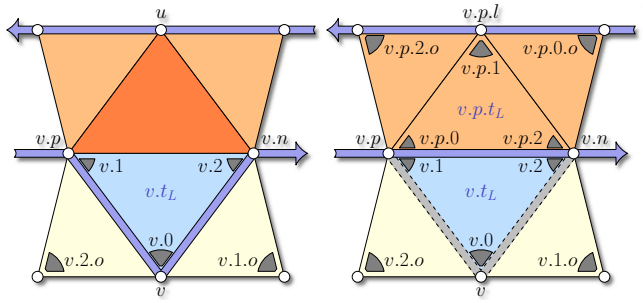

Figure 7: *Wart skipping treats T_0 triangles (red) adjacent to T_2 warts (blue) as T_1 triangles (cream/orange) by excluding the wart from the ring. The T_0 is stored as the first redundant copy of the T_2.*

If $c.o$ lies in a T_0, on the other hand, we cannot reach it via the ring, and we store in L or R a bit signaling that $c.t$ is an expensive T_1^i or T_2^i triangle. In this case, rather than storing $v.l$, we store in $L[v]$ an index into a condensed corner table VO^* (and similarly for $v.r$). VO^* holds triplets $(v.l, v.0.o, v.2.o)$ and $(v.r, v.4.o, v.6.o)$.

Finally, for corners c in T_0 triangles, we consult the O table, which holds opposites for all three corners of such triangles.

4.6 Meshes with Borders

As discussed previously, LR can handle meshes with borders by introducing triangles that join border edges to a single dummy vertex v. If there are several border loops, this addition creates non-manifold edges. We ensure that v is not a part of the ring by initially marking it as visited, which guarantees that we never invade any of the dummy triangles incident on v. Any reference to v in the LR table is replaced with a special null index.

4.7 Implementation of Operators

We summarize here the implementation of the standard operators.

c.v: If $c \geq 8m_r$, then $c.t$ is a T_0 triangle and $c.v = V[i]$, where $i = c - \lfloor c/4 \rfloor - 6m_r$. (This subtraction of $\lfloor c/4 \rfloor$ restores the base to six to avoid unused corners in the VO table.) Otherwise, we compute $v = \lfloor c/8 \rfloor$ and use the relative corner offset $c \bmod 8$ to select among v, $v.n$, $v.l$, and $v.r$ (see Fig. 5).

c.o: If $c \geq 8m_r$, then $c.t$ is a T_0 triangle and $c.o = O[i]$, where $i = c - \lfloor c/4 \rfloor - 6m_r$. Otherwise, we let $v = \lfloor c/8 \rfloor$ and distinguish several cases (Fig. 6). In the first case, $v.1.o = 8v + 5$ and $v.5.o = 8v + 1$. In the next three cases, we infer the opposite from the L and R tables and ring vertices. For example, if $v.l = v.n.l$, then $v.0.o = 8v.n + 2$. When c is in a T^i triangle, we look up $c.o$ using $v.l$ or $v.r$ as an index into the VO^* table. The other cases can be derived by symmetry.

v.c: If $v \geq m_r$, then v is isolated and $v.c = C[v - m_r]$. Otherwise, if $v.l = v.n.n$ (redundant T_2 triangle), then $v.c = 8v.n + 1$ (and similarly for $v.r$); otherwise $v.c = 8v$.

c.t: The triangle $c.t$ of corner c is defined as $\lfloor c/4 \rfloor$.

t.c: The first corner $t.c$ of triangle t is defined as $4t$.

c.n: The next operator is defined as $c.n = c - 2$ if $c \bmod 4 = 2$; otherwise $c.n = c + 1$.

c.p, **c.s**, **c.l**, and **c.r** are derived from the operators discussed above.

5 Wart Skipping

The number of T_0 triangles is typically small compared to the number of T_1 triangles. However, the connectivity information associated with a T_0 triangle requires more storage, both for itself and for its adjacent triangles. Hence, it is important to reduce the number of T_0 triangles. To do so, we identify warts: T_2 triangles that are adjacent to T_0 triangles. (When more than one T_2 triangle is adjacent to a T_0, only one of them is considered a wart.) Because each T_2 triangle is duplicated, we may reclaim the storage for the redundant copy and use it to represent the T_0. That is, for a T_2 triangle $(v.n, v, v.p)$ adjacent to a T_0 triangle $(v.p, u, v.n)$, we store u rather than $v.n$ in $L[v.p]$ (see Fig. 7). We also store a bit in the entry for the T_0 to indicate that it has been paired with a wart, and use T_0^w to denote such triangles. Warts are denoted T_2^w.

To correctly process T_0^w and T_2^w triangles, we conceptually modify the ring by skipping over the wart and its tip vertex v when accessing the T_0^w, which in effect makes $(v.p, v.n)$ a ring edge and turns the T_0^w triangle into a regular T_1 (Fig. 7). This reclassification of the T_0 also affects any incident T_1^i or T_2^i triangles, which unless they are adjacent to another T_0 now become regular (cheap) triangles.

The impact of wart skipping on the corner operators is small: For $c.v$ and $c.o$, we let $v.p.n = v.n$ and $v.n.p = v.p$ whenever accessing a T_0^w triangle. Opposites of wart tip corners are also redefined as $v.0.o = v.p.1$ and $v.6.o = v.p.5$, and conversely for T_0^w tip corners. Aside from this change, the corner operators for warts stay the same.

To appreciate the benefit of wart skipping, note that we make actual use of the redundant reference for the T_2 triangle, reduce the 6-reference cost for the T_0 triangle to a single entry, and reduce the 4-reference cost of all adjacent T_1^i and T_2^i triangles to a single entry, for a gain of as many as 15 references per skipped wart. In practice, because T_0 and T_2 triangles often come in pairs, wart skipping usually reduces the number of T_0 triangles by more than half.

6 Storage Efficient LR Representation

The LR representation discussed so far has been optimized to reduce the number of integer references per triangle. Its binary storage efficiency can be improved by carefully considering how these references are encoded. In particular, by changing the traversal of RING-EXPANDER to produce a ring with greater locality of reference, we allow short relative indices to be used even for very large meshes, though possibly using a larger *number* of references. This space-optimized representation is discussed below.

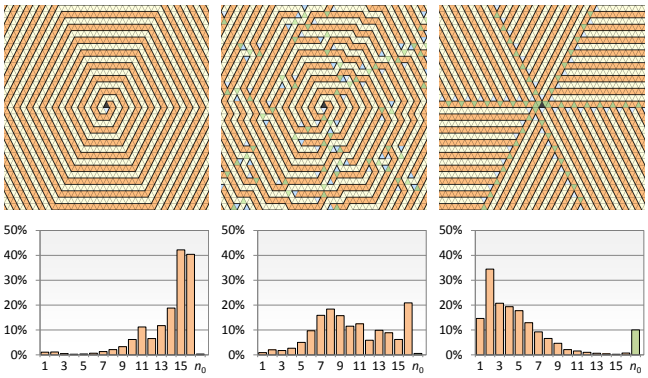

Figure 8: *Depth-first (left), hybrid $k = 32$ (middle), and breadth-first (right) traversals, with offset distributions in number of significant bits (1 to 16) and fractions of T_0 triangles (green, rightmost column), which are 0.33%, 0.56%, and 10%.*

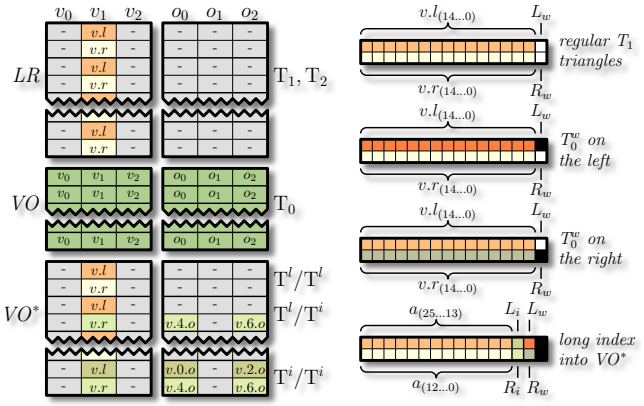

Figure 9: *Bit-efficient LR storage. Left: Each row corresponds to a triangle. Gray shaded vertices and corners are implicit and are not stored. Right: Encoding of LR table using 16 bits per reference.*

6.1 Relative Indexing

The LR table, as presented above, stores 32-bit integer references to vertices. In practice the index difference, or offset, between a ring vertex v and its left and right neighbors $v.l$ and $v.r$ is often small enough to fit in 16 bits, even when the mesh has far more than 2^{16} vertices. We exploit this and store the offsets $v.l - v$ and $v.r - v$ (modulo the number of ring vertices m_r) more compactly than the absolute indices. For large meshes, however, the depth-first traversal of RING-EXPANDER often results in very long triangle strip corridors between bifurcations (Fig. 8, left). In general, more bifurcations, and thus shorter corridors, lead to smaller offsets.

A breadth-first strategy for RING-EXPANDER (Fig. 8, right) generates shorter offsets, but favors bifurcations—i.e. expensive T_0 triangles—over long corridors—i.e. cheap T_1 triangles. Hence, we propose a compromise (Fig. 8, center): A hybrid breadth- and depth-first traversal that balances the number of bifurcations and the magnitudes of offsets. It modifies RING-EXPANDER to interrupt the depth-first traversal every k steps and resets the traversal using breadth-first backtracking. Setting, $k = 1$ results in a pure breadth-first traversal, while $k = \infty$ yields a depth-first traversal. Intermediate values of k may be used to tune the number of bifurcations and distribution of offsets.

Our HYBRID-RING-EXPANDER algorithm records backtracking corners in a double-ended queue d that is initially empty:

```
c.n.v.m = c.p.v.m = true;      // mark vertices as visited
while (true) {
    if (!c.v.m) {              // has c.v been visited?
        c.v.m = c.t.m = true; // invade c.t
        d.push_back(c.l);      // push left and right...
        d.push_back(c.r);      // ... neighbors onto deque
        n++;                   // increment triangle count
    }
    if (d.empty()) break;
    if (n % k == 0) c = d.pop_front();   // breadth-first
    else            c = d.pop_back();    // depth-first
}
```

Though slightly more complex than RING-EXPANDER, this hybrid method still achieves a throughput of 25 million triangles/second.

Rings generated with an optimal value of k tend to have offsets that can be stored as 15-bit signed integers. When this is the case for both of a pair of $v.t_L$ and $v.t_R$ triangles, we store the offsets as 16-bit entries in the LR table. LR entries that require more bits are handled using one level of indirection into the VO^* table, which is indexed by combining bits from the L and the R entries into a 26-bit reference a. VO^* stores the corresponding $v.l$ and $v.r$ indices in consecutive locations $VO^*[a]$ and $VO^*[a+1]$ using 32 bits each. We use T^l to identify triangles that require this extra level of indirection and specification of $v.l$ or $v.r$ using **long references**. As in standard LR, T^i denotes irregular triangles adjacent to a T_0 that also require long indexing into VO^*, for which one vertex and two opposite corners are stored.

One may think of the VO^* table as a full corner table, but with references that are already known removed (see Fig. 9). Our implementation discards the unused VO^* entries and packs this table into a single linear array of integer references. Because we always arrive at a sequence of entries in this table knowing the type of each triangle in a pair—$\mathrm{T}^l/\mathrm{T}^l$, $\mathrm{T}^l/\mathrm{T}^i$, $\mathrm{T}^i/\mathrm{T}^l$, or $\mathrm{T}^i/\mathrm{T}^i$—there is no ambiguity what the next 2, 4, or 6 integer entries represent. In particular, the first two references of a tuple always store $v.l$ and $v.r$.

6.2 Storage Format

For each LR entry we store two bits, L_w and R_w, identifying one of four configurations: a pair of T_1 triangles, a T_0^w on the left or on the right, or a pair of T^l or T^i triangles that require long indexing. Note that T_0^w triangles can appear on the left or right, but not both simultaneously, as the triangle paired with the T_0^w triangle is adjacent to a T_2^w triangle and has at least one ring edge. Thus, the two bits stored in the LR table indicate whether to skip warts on the left and on the right, with the unused double-wart combination signaling the need for a long index (see Fig. 9).

As discussed above, when necessary, we combine the LR entries into a 26-bit index a into the VO^* table. With two additional bits out of the 32 already used, the remaining four bits are used to encode left and right wart skips (since a triangle may require a long index into the VO^* table *and* a wart skip) and whether $v.t_L$ and/or $v.t_R$ is adjacent to a T_0, i.e. if it is an irregular T^i.

The VO table stores first a list of all T_0 triangles as six references per triangle. Any subsequent vertices and opposite corners that cannot be represented directly in the LR table are stored as variable-length records, in no particular order, in the VO^* table. The index a and the combination of L_i and R_i bits, which distinguish T from T^i triangles, are sufficient to determine the record type.

mesh	n	%v6	standard LR					SQuad	bit-efficient LR						
			m_i	$\%T_0$	$\%T_0^w$	$\%T^i$	rpt	rpt	k	m_i	$\%T_0$	$\%T_0^w$	$\%T^l$	$\%T^i$	bpt
bunny	69,451	75.1	1	0.41	1.74	1.14	1.062	2.054	226	1	0.63	1.49	3.94	1.81	20.27
rocker arm	80,354	65.2	0	0.39	1.73	1.06	1.055	2.054	720	0	0.40	1.79	1.71	1.10	18.37
horse	96,966	66.5	1	0.39	1.48	1.05	1.055	2.046	226	0	0.61	1.53	8.61	1.72	21.59
dinosaur	112,384	57.9	0	0.75	2.30	2.02	1.106	2.072	106	3	1.35	2.34	12.83	3.66	26.21
armadillo	345,944	52.6	3	0.52	2.42	1.41	1.074	2.069	89	10	1.26	2.51	13.72	3.44	26.12
hand	654,666	53.4	11	1.17	3.15	3.12	1.164	2.096	68	16	1.92	3.21	28.84	5.15	33.86
buddha	1,087,716	32.1	180	4.26	3.57	10.95	1.583	2.150	38	273	4.78	3.57	26.12	12.22	45.26
welsh dragon	2,210,378	86.7	4	0.14	0.82	0.38	1.020	2.027	100	5	0.87	1.05	18.84	2.52	26.12
thai statue	10,000,000	44.4	241	1.85	3.12	4.96	1.260	2.111	69	298	2.39	3.12	23.73	6.42	34.35
david	55,514,795	51.6	1143	0.63	3.19	1.64	1.089	2.082	108	1623	1.21	3.10	23.06	3.28	28.89

Table 1: *Left: Storage statistics for the standard and bit-efficient LR representation. Right: Meshes color-coded blue-to-red in ring order.*

7 LR for Efficient Rendering

Although our LR representation was primarily designed to support efficient mesh connectivity queries, a leaner version that does not store corner pointers may find utility in any number of applications that require only a representation of a static indexed triangle list. Three such applications include efficient offline or in-memory storage, transmission, and high-throughput rendering.

At its heart, the LR table encodes a coherent sequence of vertices and triangles. As such, it makes for a lean indexed mesh representation with exactly one vertex reference per triangle; the ring vertices are consecutive and need not be specified. (The few T_0 triangles may be represented verbatim.) This simple representation suggests the possibility of using LR as an efficient rendering primitive.

The LR representation directly rivals the common *triangle strip*. Each branch in one of the interlocking LR triangle trees can be thought of as a generalized triangle strip. Whereas a typical mesh can be represented as a collection of (non-generalized) triangle strips using about 1.35 references per triangle, LR requires only one reference per triangle, and avoids the overhead associated with strip "swaps" or "restarts." In addition to being more space efficient, our LR mesh is easier and faster to construct than triangle strips, which require greedy or more complex construction procedures. As an example, our RING-EXPANDER method is two orders of magnitude faster than Evans et al.'s [1996] *Stripe* software.

Efficient rendering is possible by "decompressing" the LR representation on the fly, e.g., using a geometry shader, into indexed triangles that reference a vertex buffer object (VBO). This allows storing a compressed index list on the GPU that omits the implicit consecutive ring vertex indices. We may maximize locality of reference for the GPU post-transform-and-lighting vertex cache by using a breadth-first LR construction. As in the standard LR representation, wart skips can be encoded using a dedicated bit that is set only for T_0^w triangles. Duplicates of T_2 triangles and non-existent triangles across mesh borders can be eliminated by specifying either v or $v.n$ as the tip vertex, which both result in degenerate triangles.

8 Results

We report in Table 1 statistics for several benchmark models. Let the mesh have m vertices, n triangles, and a ring with m_r vertices, leaving $m_i = m - m_r$ vertices isolated. Let n_0 be the number of T_0 triangles remaining after wart skipping, and let n^i be the number of T_1^i and T_2^i triangles. In the standard LR representation, we store a total of $2m_r$ references in the LR table, $6n_0$ references in the VO table, $3n^i$ references in the VO^* table, and m_i references in the C table. Hence, the storage cost for the standard LR representation is $2m_r + 6n_0 + 3n^i + m_i$ references, which is **1+f rpt**, where f is about $(6n_0 + 3n^i - m_i)/(2m)$, assuming $n \simeq 2m$.

For the bit-efficient LR, we store 16-bit references in the L and R tables, while the other tables hold 32-bit references. Hence, the total storage cost in bits is $32(m_r + 6n_0 + 3n^i + n^l + m_i)$, where n^l denotes the number of T_1^l and T_2^l triangles.

Table 1 reports for the standard LR representation the number of triangles n and isolated vertices m_i, the percentage of valence-6 vertices and T_0, T_0^w, and T^i triangles, as well as the resulting rpt. The median rpt for LR is **1.08 rpt**, which is about half the storage cost for SQuad. As in SQuad, the storage cost is influenced by the regularity of the mesh, and increases with fewer valence-6 vertices.

For the bit-efficient representation, we also report the period k between breadth-first restarts, the percentage of T^l triangles, and the resulting number of bits per triangle (bpt). The median is **26.2 bpt**. We ran the construction several times and chose the k that resulted in the lowest storage cost. Given that we can construct LR meshes from corner tables at a rate of two million triangles per second, we can afford to explore several k values and seed corners per mesh.

Fig. 10 shows the access time for processing the 55 million triangle David mesh using CT [Rossignac 2001], SQuad [Gurung et al. 2011], and the standard LR using various memory configurations. (Our unoptimized implementation of the bit-efficient LR is on average five times slower than standard LR.) Note that the operating system reserves at least 400 MB for system purposes and, hence, we are left with the remaining memory. Using sequential loops over corners and vertices, we report timings for $c.v$, $c.o$ (for LR and CT) or $c.s$ (for SQuad), and for operations that compute the valence and normal of a vertex. As in [Gurung et al. 2011], we also report the cost per triangle traversed when following the "contour" where the mesh intersects a plane, which involves a non-sequential, data-dependent traversal.

Although the sequential $c.v$ and $c.o$ table lookups in CT are faster than the computations needed by LR when the mesh fits in main memory, this performance difference is not observed when considering higher-level tasks that require some level of random access, e.g. to access neighboring vertices. In this case LR is generally *faster* than both CT and SQuad due to its smaller memory footprint and improved cache utilization. Furthermore, because the storage needed by LR for most meshes is about half the storage needed by SQuad, and about 1/6 the storage of CT, LR is significantly faster than CT and SQuad when processing large models that do not fit in main memory, because the reduced storage leads to fewer page faults.

Finally, we evaluated the number of references per triangle needed for a renderable indexed mesh representation of LR (i.e. with corner references removed). Using a depth-first traversal with wart skips, the mean storage required is 1.03 rpt, which increases to 1.10 rpt when wart skips are disallowed. This compares favorably with Stripe, which requires 1.35 rpt on average.

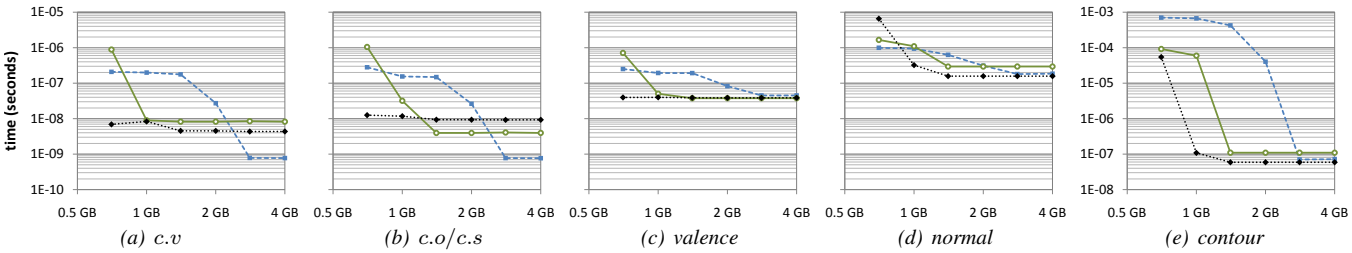

(a) c.v *(b) c.o/c.s* *(c) valence* *(d) normal* *(e) contour*

Figure 10: *Per-element execution time versus available main memory for CT (dashed blue), SQuad (solid green), and LR (dotted black).*

8.1 Limitations

Because LR stores vertex references in a contiguous memory array, and because inserting an array entry would require updating many of the indices in this array, incremental connectivity changes cannot be performed efficiently. We recommend LR for use in applications where mesh connectivity remains fixed, or where constructing a new LR with the desired connectivity is acceptable.

Our construction algorithm assumes as input a mesh data structure such as the corner table (CT) that provides constant-time adjacency queries. A CT can be constructed from a set of indexed triangles in linear time, but the memory overhead of keeping both the CT and LR in memory at the same time may be unacceptable.

9 Conclusion

We have described a simple and efficient implementation of the LR data structure for representing the connectivity of manifold triangle meshes. It supports a comprehensive set of constant-time, random-access operators for traversing the mesh and offers roughly the same performance as the best previously reported solution, SQuad. Yet LR requires only about half of the storage needed by SQuad, namely about **1.08 references per triangle**, or, with the bit-efficient variation, only about **26.2 bits per triangle**. Hence, LR requires about 6 times less storage than the corner table and 9 times less than the winged-edge representation.

References

ARKIN, E. M., HELD, M., MITCHELL, J. S. B., AND SKIENA, S. S. 1996. Hamiltonian triangulations for fast rendering. *The Visual Computer 12*, 9, 429–444.

BAUMGART, B. G. 1972. Winged edge polyhedron representation. Tech. Rep. CS-TR-72-320, Stanford University.

BLANDFORD, D. K., BLELLOCH, G. E., CARDOZE, D. E., AND KADOW, C. 2005. Compact representations of simplicial meshes in two and three dimensions. *International Journal of Computational Geometry and Applications 15*, 1, 3–24.

BRISSON, E. 1989. Representing geometric structures in d dimensions: Topology and order. In *ACM Symposium on Computational Geometry*, 218–227.

CAMPAGNA, S., KOBBELT, L., AND SEIDEL, H.-P. 1998. Directed edges—A scalable representation for triangle meshes. *Journal of Graphics Tools 3*, 4, 1–11.

CASTELLI ALEARDI, L., DEVILLERS, O., AND MEBARKI, A. 2006. 2D triangulation representation using stable catalogs. In *Canadian Conference on Computational Geometry*, 71–74.

CASTELLI ALEARDI, L., DEVILLERS, O., AND SCHAEFFER, G. 2006. Optimal succinct representations of planar maps. In *ACM Symposium on Computational Geometry*, 309–318.

COURBET, C., AND HUDELOT, C. 2009. Random accessible hierarchical mesh compression for interactive visualization. In *Symposium on Geometry Processing*, 1311–1318.

EVANS, F., SKIENA, S., AND VARSHNEY, A. 1996. Optimizing triangle strips for fast rendering. In *IEEE Visualization*, 319–326.

GOPI, M., AND EPPSTEIN, D. 2004. Single-strip triangulation of manifolds with arbitrary topology. *Computer Graphics Forum 23*, 3, 371–379.

GUIBAS, L., AND STOLFI, J. 1985. Primitives for the manipulation of general subdivisions and the computation of Voronoi diagrams. *ACM Transactions on Graphics 4*, 2, 74–123.

GURUNG, T., LANEY, D., LINDSTROM, P., AND ROSSIGNAC, J. 2011. SQuad: Compact representation for triangle meshes. *Computer Graphics Forum 30*, 2, 355–364.

KALLMANN, M., AND THALMANN, D. 2001. Star-vertices: A compact representation for planar meshes with adjacency information. *Journal of Graphics Tools 6*, 1, 7–18.

KHODAKOVSKY, A., ALLIEZ, P., DESBRUN, M., AND SCHRÖDER, P. 2002. Near-optimal connectivity encoding of 2-manifold polygon meshes. *Graphical Models 64*, 3–4, 147–168.

MANTYLA, M. 1988. *Introduction to Solid Modeling*. W. H. Freeman & Co.

MEBARKI, A. 2008. *Implantation de structures de données compactes pour les triangulations*. PhD thesis, Université de Nice-Sophia Antipolis.

ROSSIGNAC, J., AND CARDOZE, D. 1999. Matchmaker: Manifold BReps for non-manifold r-sets. In *ACM Symposium on Solid Modeling and Applications*, 31–41.

ROSSIGNAC, J. 1994. Through the cracks of the solid modeling milestone. In *From object modelling to advanced visualization*. Springer Verlag, 1–75.

ROSSIGNAC, J. 1999. Edgebreaker: Connectivity compression for triangle meshes. *IEEE Transactions on Visualization and Computer Graphics 5*, 1, 47–61.

ROSSIGNAC, J. 2001. 3D compression made simple: Edgebreaker with zip&wrap on a corner-table. In *International Conference on Shape Modeling & Applications*, 278–283.

SNOEYINK, J., AND SPECKMANN, B. 1999. Tripod: A minimalist data structure for embedded triangulations. In *Computational Graph Theory and Combinatorics*.

UPADHYAY, A. K., 2010. Contractible Hamiltonian cycles in triangulated surfaces. http://arxiv.org/pdf/1003.5268.

YOON, S.-E., AND LINDSTROM, P. 2007. Random-accessible compressed triangle meshes. *IEEE Transactions on Visualization and Computer Graphics 13*, 6, 1536–1543.